Finite-size corrections for confined polymers in the extended de Gennes regime

Toby St Clere Smithe, Vitalii Iarko, Abhiram Muralidhar, Erik Werner, Kevin D. Dorfman, and Bernhard Mehlig

Phys. Rev. E **92**, 062601 — Published 17 December 2015

DOI: 10.1103/PhysRevE.92.062601

Finite-size corrections for confined polymers in the extended de Gennes regime

T. St Clere Smithe,[1] V. Iarko,[1] A. Muralidhar,[2] E. Werner,[1,*] K. D. Dorfman,[2] and B. Mehlig[1]

[1] *Department of Physics, University of Gothenburg, Origovägen 6B, 412 96 Göteborg, Sweden*
[2] *Department of Chemical Engineering and Materials Science, University of Minnesota – Twin Cities, 421 Washington Avenue SE, Minneapolis, Minnesota 55455, USA*

Theoretical results for the extension of a polymer confined to a channel are usually derived in the limit of infinite contour length. But experimental studies and simulations of DNA molecules confined to nanochannels are not necessarily in this asymptotic limit. We calculate the statistics of the span and the end-to-end distance of a semiflexible polymer of finite length in the extended de Gennes regime, exploiting the fact that the problem can be mapped to a one-dimensional weakly self-avoiding random walk. The results thus obtained compare favourably with pruned-enriched Rosenbluth method (PERM) simulations of a three-dimensional discrete wormlike chain model of DNA confined in a nanochannel. We discuss the implications for experimental studies of linear λ-DNA confined to nanochannels at the high ionic strengths used in many experiments.

PACS numbers: 36.20.Ey, 87.15.A-, 05.40.Fb, 87.14.gk

I. INTRODUCTION

The extension statistics of semiflexible polymers confined to channels have been studied in great detail during the last years [1–15]. A large number of scaling laws have been identified, valid at different values of the physical parameters describing the polymer and the strength of confinement. (See Ref. [16] for an overview describing the different regimes of extensional fluctuations of a polymer in a rectangular channel.) But these scaling laws are strictly valid only in the limit where the contour length L of the polymer tends to infinity, and experiments and simulations may not correspond to the asymptotic limit. Therefore it is important to understand to what extent these results apply for finite contour lengths, and how they must be corrected to accurately describe the statistics obtained in experiments at finite values of L.

This motivated us to compute the finite-size corrections of the mean values and variances of the end-to-end distance and the span of confined polymers in the 'extended de Gennes regime' [17]. In this regime we can make use of recent results [11] that show how the conformational statistics of the confined polymer can be mapped to a one-dimensional model. This allows us to analyse finite-size corrections in two ways. First, a scaling law determines the magnitude of the finite-size corrections as a function of the physical parameters. Second, Monte-Carlo simulations of the one-dimensional model allow us to compute this scaling function to a high degree of accuracy. We show that the finite-size effects produced by this one-dimensional model provide a reasonably accurate description of detailed three-dimensional simulations of a confined, discrete wormlike chain model of DNA in a high ionic-strength buffer. Finally we show that finite-size effects are of experimental importance, by estimating the magnitude of the finite-size corrections for the statistics of the end-to-end distance of λ-DNA confined to nanochannels.

There are only limited data in the literature concerning finite-size effects for confined DNA. In simulations, Muralidhar *et al.* [10] estimated finite-size corrections for the extension of DNA confined to square channels of widths between 30 and 400 nm at high ionic strength for contour lengths out to the asymptotic limit, corresponding to almost 10^4 persistence lengths for the largest channel size. This analysis took advantage of pruned-enriched Rosenbluth method simulations (PERM) [18, 19] of a discrete wormlike chain model consisting of a semiflexible chain of touching beads. PERM is especially well suited to study finite-size effects, as it natively produces data as a function of molecular weight while avoiding the attrition problems due to excluded volume between segments of the chain and between the chain and the walls. Muralidhar *et al.* [10] found the span of λ-DNA to be within 3% of the value in the infinite-L limit, for the buffer strengths and channel dimensions they studied in their paper.

The study of finite-size effects is especially important in light of recent work comparing experimental data on nanochannel-confined DNA to simulations [9, 14] and theory [14, 20]. Simulations and theoretical predictions using reasonable values of the physical properties of DNA are within around 10% of the experimental results. The remaining disagreement between theory/simulation and experiment arises in part due to uncertainties in the theories used to estimate the persistence length [21, 22] and effective width [20, 23] of the polymer, which are required inputs to the model, as well as experimental artifacts that lead to molecular weight dispersity [14], such as heterogeneous staining [24], photocleavage [25], or shear cleavage [26], that may not be controlled in all experiments. However, for λ-DNA the finite-size effects are of a similar order of magnitude to the aforementioned sources of error [10]. In the following we explain how the finite-size effects depend on the parameters describing the confined DNA. As a result, we anticipate that the results described below will prove very useful in future quantitative comparisons

* erik.werner@physics.gu.se

between theory and experiment for DNA.

II. EXTENDED DE GENNES REGIME

For a semiflexible polymer of Kuhn length $\ell_{\rm K}$ and effective width $w_{\rm eff} \ll \ell_{\rm K}$ confined to a square channel of cross section $D \times D$, the extended de Gennes regime is defined by the conditions [7, 8, 11, 17, 27]

$$\ell_{\rm K} \ll D \ll \ell_{\rm K}^2/w_{\rm eff}. \tag{1}$$

In the extended de Gennes regime it is possible to map the statistics of the channel-confined polymer to those of a one-dimensional weakly self-avoiding random walk [11]. In its simplest form, this one-dimensional walk is given by a simple random walk on $\mathbb{Z}$, but with an energy penalty whenever two steps of the random walk land on the same site. The model is therefore defined by two parameters: the total number N of steps taken, and the energy penalty ϵ (measured in units of $k_{\rm B}T$). The mapping shows that the energy penalty is related to the overlap probability of two polymer segments which are in the same section of the channel [11]. In terms of the parameters of the confined polymer it is given by

$$\varepsilon = \frac{9\sqrt{3}\pi}{8}\beta, \tag{2}$$

where the scaling factor β is defined as

$$\beta = \frac{\ell_{\rm K} w_{\rm eff}}{D^2}\,. \tag{3}$$

It follows from Eqs. (1)-(3) that $\varepsilon \ll 1$ in the extended de Gennes regime. In this limit, results for this one-dimensional model can be directly translated into predictions for the confined semiflexible polymer if each step of the random walk is interpreted as one Kuhn-length segment of the polymer, and the lattice spacing of the one-dimensional model corresponds to a distance $\ell_{\rm K}/\sqrt{3}$ in the channel direction. Although in this paper we only consider macroscopic observables we emphasise that the mapping holds also for microscopic observables, provided that one considers contour-length separations significantly larger than one Kuhn length.

Two common measures of the extension of a channel-confined polymer are the end-to-end distance $r = |z(L) - z(0)|$ and the span $R = \max_s z(s) - \min_s z(s)$. Here z denotes the coordinate along the channel axis, and s parameterises the contour length of the polymer. This parameter ranges between 0 and L. The mapping to a one-dimensional weakly self-avoiding random walk leads to exact predictions for the equilibrium distributions of r and R [28]. In particular, in the limit $L \to \infty$, the first two moments of the equilibrium distributions for R and r are identical and obey [11]

$$\mu_r = \mu_R = 0.9338(84)\, L \left(\frac{\ell_{\rm K} w_{\rm eff}}{D^2}\right)^{1/3}, \tag{4}$$

$$\sigma_r^2 = \sigma_R^2 = 0.133(12)\, L\ell_{\rm K}\,. \tag{5}$$

The errors quoted in these equations reflect mathematical bounds [11] derived from the exact results of Ref. [28].

The question posed in the Introduction is: how much do these observables deviate from the above scaling predictions when L is finite? In the extended de Gennes regime the finite-size analysis is simplified by a universal scaling relation [11] implying that all observables must collapse onto a universal curve when plotted as functions of the scaled variables

$$L' = (L/\ell_{\rm K})\beta^{2/3}, \quad z' = (z/\ell_{\rm K})\beta^{1/3}\,. \tag{6}$$

Here L is the contour length. The scaling law derives from a corresponding scaling law for the one-dimensional model in the limit $\varepsilon \to 0$: $n' = n\varepsilon^{2/3}$ and $z' = z\varepsilon^{1/3}$ where n is the number of steps and z is the distance traversed by the random walk [11].

III. SIMULATION METHODS

A. 1D weakly self-avoiding random walk

In order to determine how μ_r, μ_R, σ_r^2 and σ_R^2 differ from the asymptotic results (4) and (5), we compute these properties as functions of N in simulations. Because of the scaling property (3) it suffices to perform simulations for a single value of ε. We here use the value $\varepsilon = 0.0011$. We have verified that this number is sufficiently small for the observables to obey the scaling to good accuracy. The simulations employ a chain-growth method with a fixed number of chains at each contour length, as described in Ref. [8]. The method can be summarised as follows.

The configuration for a given chain is generated by taking one step at a time on a one-dimensional lattice, up to a maximum number of steps. A step is made with equal probability in either direction along the lattice. Random walks that revisit previously visited sites are penalised as follows. Assume that after step j is made the random walk lands on a site that has already been visited τ times (where τ is known as the local time [28]). The chain growth continues to step $j+1$ with probability $p = \exp(-\varepsilon\tau)$ and the growth is terminated at step j with probability $1-p$.

Walks are generated in batches of constant size N_c, until a total of $N_t = 200$ million walks are produced. The initial statistical weight for each chain k is then $w_1^{(k)} = 1/N_t$. Each iteration consists of making one step for each walk in the batch. The length-dependent averages and standard deviations for the end-to-end distance are computed as the weighted values

$$\mu_r(j) = Z_j^{-1} \sum_{k=1}^{N_t} w_j^{(k)} r_j^{(k)}, \tag{7}$$

$$\sigma_r^2(j) = Z_j^{-1} \sum_{k=1}^{N_t} w_j^{(k)} [r_j^{(k)} - \mu_r(j)]^2, \tag{8}$$

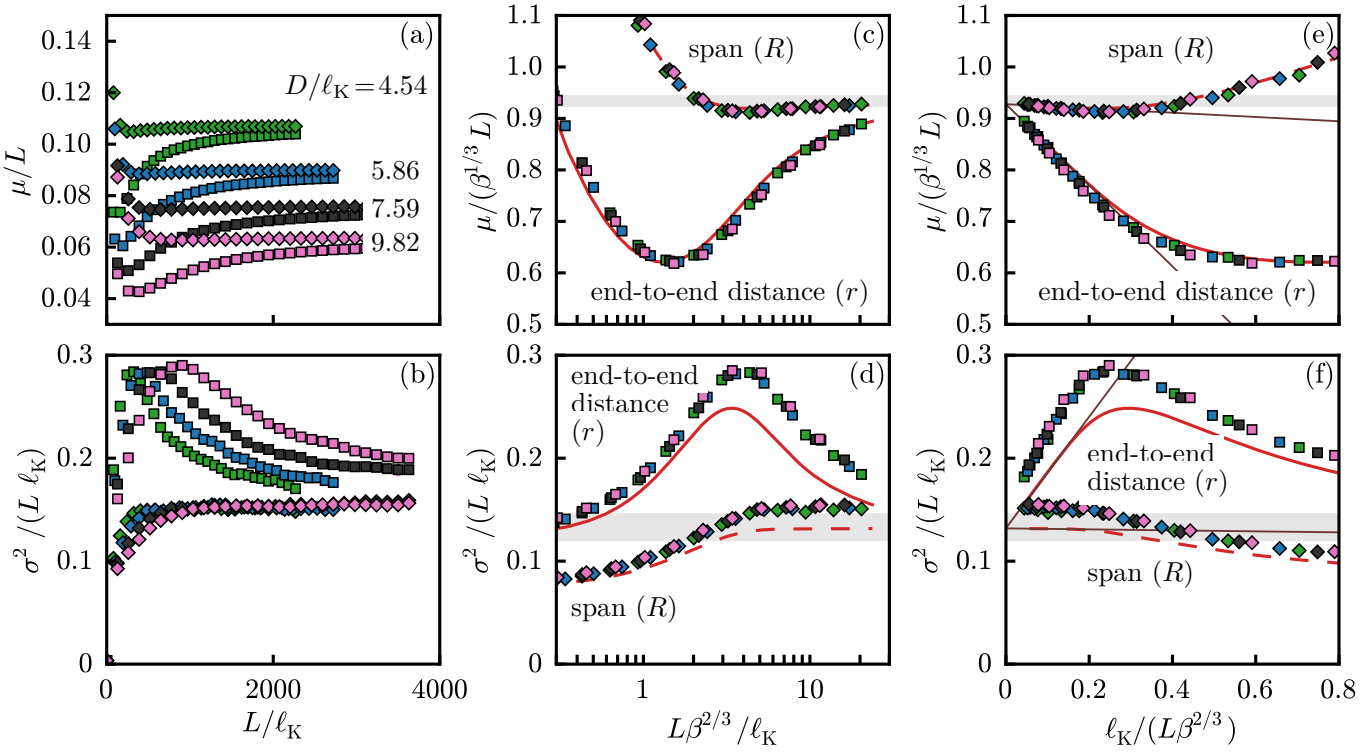

FIG. 1. (a), (b) Mean and variance of the end-to-end distance r and span R of a discrete wormlike chain model of DNA in a high ionic-strength buffer ($d = 4.6$ nm, $\ell_K = 101.4$ nm) confined in a channel of width D as a function of contour length L. Symbols show results from three-dimensional simulations of the discrete wormlike chain model, for channel widths $D/\ell_K = 9.82$ (pink), $D/\ell_K = 7.59$ (grey), $D/\ell_K = 5.86$ (blue) and $D/\ell_K = 4.54$ (green, $\square$ for r, $\diamond$ for R). (c),(d): Same data, rescaled according to Eqs. (3) and (6) with $w_{\text{eff}} = d/1.45$ (see text). The grey shaded areas denote the asymptotic predictions of Eqs. (4) and (5) in the limit $\beta \to 0$ and $L \to \infty$. Lines show the results from the one-dimensional model for a small value of ε ($\varepsilon = 0.0011$). Solid lines for r, dashed for R. Panels (e) and (f) are as (c) and (d), except now as a function of $1/L$ to emphasise the linear dependence on $(L\beta^{2/3})^{-1}$ in the limit of $L \to \infty$ (thin brown lines show this extrapolation).

with equivalent expressions for the span R using all surviving walks at step j. $Z_j = \sum_k w_j^{(k)}$ is the estimate of the partition function after j steps. If N_p configurations are terminated at step j, then we randomly select N_p of the surviving chains and make copies of these chains. All of the statistical weights are then updated as

$$w_j^{(k)} = w_{j-1}^{(k)} \left(\frac{N_c - N_p}{N_c} \right), \tag{9}$$

Note that under this update scheme all weights in a given batch are identical, yet weights differ between batches.

B. Discrete wormlike chain model

We also compare the results from the mapping of the weakly self-avoiding random walk to detailed simulations of a discrete wormlike chain confined in a nanochannel. With an eye towards applications to experiments, we chose reasonable parameters for DNA at high ionic strength, using $N+1$ touching beads of diameter $d = 4.6$ nm, with contour length L and Kuhn length $\ell_K = 101.4$ nm. The centre of each bead is constrained to lie within a channel with a square cross section of width D. Self-avoidance is imposed by disallowing configurations where the distance between the centres of any two beads is less than d. Beads are connected by rigid bonds, and stiffness is imposed by the bending potential

$$U(\theta_1, \ldots, \theta_N) = k_B T \kappa \sum_{n=1}^{N-1} (1 - \cos\theta_n), \tag{10}$$

where n is a bond index, θ_n is the angle between bonds n and $n+1$, and κ is the 'bending constant' [10]. The Kuhn length is given by

$$\ell_K = d \sum_{k=-\infty}^{\infty} \langle \boldsymbol{t}_n \boldsymbol{t}_{n+k} \rangle, \tag{11}$$

where $\boldsymbol{t}_n$ is the unit tangent vector to the chain backbone. This definition leads to the relationship [29, 30]

$$\frac{\ell_K}{d} = \frac{\kappa + \kappa \coth(\kappa) - 1}{\kappa - \kappa \coth(\kappa) + 1} \approx 2\kappa - 1\,. \tag{12}$$

The approximation is excellent for chains as stiff as the ones considered here. Simulations of the discrete wormlike chain model use the pruned-enriched Rosenbluth

method (PERM) following the approach described in detail in Refs. [10, 31]. The simulation data here consist of 1.8 million tours in total for each channel size.

IV. RESULTS AND DISCUSSION

Figure 1 presents numerical results of the simulations described above. Panels (a) and (b) show the finite-size corrections for the means and variances of the span and the end-to-end distance for the discrete wormlike chain model of confined DNA. We see that the magnitude of the finite-size corrections depends not only on L but also the channel size D and on the observable in question. In comparing the weakly self-avoiding random walk to the detailed simulation data, it is important to keep in mind that Eqs. (4) to (6) are valid for arbitrary polymer models provided that $w_{\rm eff}$ is *defined* in terms of the excluded volume v of a Kuhn length segment as $v = (\pi/2)\ell_{\rm K}^2 w_{\rm eff}$ [11]. This formula is valid for slender stiff cylindrical rods of width $w_{\rm eff} \ll \ell_{\rm K}$ [32]. But we cannot calculate $w_{\rm eff}$ because the excluded volume v is not known for the discrete wormlike chain model: the fact that the polymer is represented as a chain of touching beads complicates the geometrical analysis. A second complicating factor is that the Kuhn-length segments are not straight, this must affect the excluded volume. We therefore choose $w_{\rm eff}/d$ so that it gives the best fit between the one-dimensional model and the worm-like chain data for μ_r and μ_R. We find $w_{\rm eff}/d = 1/1.45$ for $D/\ell_{\rm K} = 5.61$ and use the same ratio for the other channel sizes.

Panels (c) and (d) of Fig. 1 demonstrate the predicted universal form of the finite-size corrections. We see that by rescaling the data according to Eqs. (3) and (6) the curves for different physical parameters collapse onto one universal curve determined by the one-dimensional random-walk model.

For the means the agreement is excellent, for the variances less so. There are two plausible reasons for this. Firstly, since $D \gg \ell_{\rm K}$ holds only approximately for the smaller channel sizes used here ($D/\ell_{\rm K} = 4.54,\ 5.86$), the polymer has a tendency to align with the channel which causes the variance to increase [33]. Indeed, as we approach the small-channel side of the extended de Gennes regime, this alignment effect and the corresponding effect on the variance becomes very strong [34]. Secondly, $D \ll \ell_{\rm K}^2/w_{\rm eff}$ holds only approximately for the bigger channel sizes ($D/\ell_{\rm K} = 7.59,\ 9.82$ corresponds to $\ell_{\rm K}^2/(Dw_{\rm eff}) = 4.21,\ 3.25$), and the variance is expected to increase when this inequality is not strongly satisfied [7]. Thus, our results suggest that for DNA in a high ionic-strength buffer the modest separation of length scales between $\ell_{\rm K}$ and $w_{\rm eff}$ means that the measured variance agrees with the theoretical prediction (5) to within 10% at best.

Panels (e) and (f) of Fig. 1 demonstrate that the finite-size corrections are of order L^{-1} in the limit of large values of L (straight lines in this limit). Extrapolation to $L \to \infty$ yields results consistent with Eqs. (4) and (5), which are indicated by the grey shaded regions of the figure. Finally, finite-size corrections to both the mean and the variance of the span are seen to be much smaller than those for the end-to-end distance, as noted in Ref. [10]. In all cases we observe that $\mu_r < \mu_R$, as expected. But for the variances the relation is instead $\sigma_r > \sigma_R$. The latter observation results from the form of the distributions for the end-to-end distance and the span as the chain size increases. While both distributions eventually converge for infinite chain lengths [10], for finite chains the width of the distribution for the end-to-end distance is wider than the distribution for the span since the ends of the chains can fluctuate within the outermost blobs.

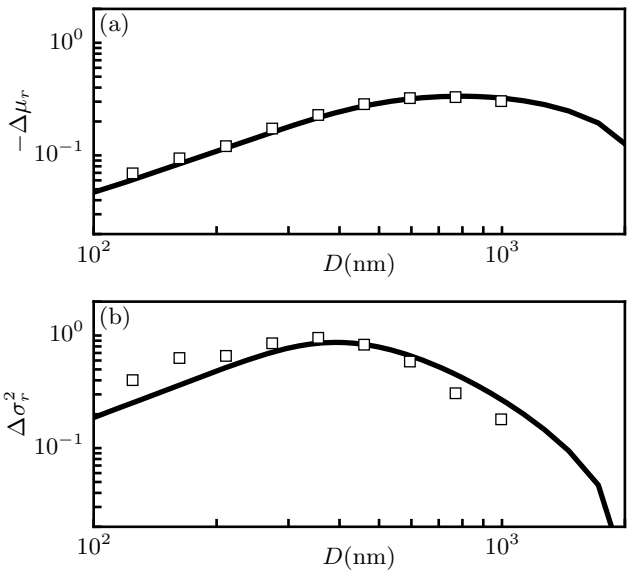

FIG. 2. Finite-size corrections in Eq. (13) for the end-to-end distance r for a model of λ-DNA in channels of different widths D. Panel (a) shows the corrections for the mean μ_r (note the minus sign), and panel (b) shows the corrections for the variance σ_r^2. Results for discrete wormlike chain model describing λ-DNA ($d = 4.6$ nm, $\ell_{\rm K} = 101.4$ nm, $L = 16$ μm) as a function of channel width D (symbols). Simulations of the one-dimensional random-walk model (solid lines).

Interestingly, the curves describing the moments of the end-to-end distance are strongly non-monotonic. For the mean, end-to-end distance, this behaviour was reported already in Ref. [10]. It is readily explained by the fact that at small values of $L' = L\beta^{2/3}/\ell_{\rm K}$ the polymer is not influenced by self-avoidance, therefore μ_r/L decreases as $L^{-1/2}$. When $L' \approx 1$, self-avoidance begins to influence the statistics, at which point μ_r/L increases, approaching the asymptotic value given by Eq. (4). By contrast, we do not know at present why the fluctuations of r increase rapidly for $L' \approx 1$. Note however that the non-monotonocity refers to the normalised observables μ_r/L, σ_r^2/L. The unscaled mean and variance are both monotonically increasing functions of L.

We conclude our discussion by estimating how important finite-size effects are for λ-DNA in the extended de Gennes regime. To this end we define the finite-size correction Δ_X of an extensive observable X as

$$\Delta_X \equiv \frac{X/L}{\lim\limits_{L\to\infty} X/L} - 1\,. \tag{13}$$

Fig. 2 shows the finite-size corrections for the mean (a) and the variance (b) of the end-to-end distance r for λ-DNA ($L = 16\,\mu$m) as a function of channel size D. Symbols show the results of the simulations of the three-dimensional discrete wormlike chain, using the data in Fig. 1(a,b), and Eq. (13). To estimate $\lim\limits_{L\to\infty} X/L$ we used the mean and the variance of the span for the largest values of L available. As mentioned above, the mean and variance of the span converge more rapidly but to the same limit as those of the end-to-end distance. Results for the one-dimensional random-walk model are shown as solid lines, obtained from the red solid lines in Fig. 1(c,d). Using Eqs. (2) and (3) we convert x-axis values in Fig. 1(c,d) to channel width D, with $\varepsilon = 0.0011$ and $w_{\text{eff}} = d/1.45 = 3.17$ nm; note that one can use any value of $\varepsilon \ll 1$ since there is a scaling relationship. We estimate the limit $\lim\limits_{L\to\infty} X/L$ by extrapolation.

We find good agreement between the two models for the mean of the end-to-end distance, with some disagreement for the variance (discussed above). It is remarkable that there is good agreement between the theory and the simulations even for small values of D, which correspond to the border of the extended de Gennes regime ($D \approx \ell_{\text{K}}$).

We see that the non-monotonicity exhibited in Fig. 1 is reflected in Fig. 2. The finite-size corrections for the mean of the end-to-end distance can be as large as 34%. The corresponding corrections for the variance are even larger, reaching 87% for $D \approx 400$ nm.

We do not show the corresponding results for the span since the finite-size corrections in this case are much smaller, and thus both of less interest and more difficult to estimate reliably.

V. CONCLUSIONS

We have estimated finite-size corrections for the extension statistics of a confined semiflexible polymer of finite length L in the extended de Gennes regime. In this regime the problem can be mapped to a one-dimensional weakly self-avoiding random walk, yielding universal scaling relations that determine the finite-size corrections.

We confirm the scaling predictions by simulations of a discrete wormlike chain model. These simulations were performed for values of Kuhn length ℓ_{K} and w_{eff} chosen to approximate those of DNA at high ionic strength. For the important special case of λ-DNA confined to a nanochannel, we find that the mean and variance of the end-to-end distance differs substantially from the asymptotic prediction as $L \to \infty$.

We emphasise that the scaling relation (3) valid in the extended de Gennes regime allows one to apply the results also for other values of ℓ_{K} and w_{eff}, as long as the channel size D satisfies the conditions (1) defining the extended de Gennes regime. Similarly, the results are easily generalisable to rectangular channels of dimensions $D_{\text{W}} \times D_{\text{H}}$ by using an effective channel size $D = \sqrt{D_{\text{W}} D_{\text{H}}}$ in Eq. (6). Note however that the conditions defining the extended de Gennes regime for rectangular channels differ from Eq. (1) [16].

This article considers semiflexible polymers in the extended de Gennes regime. It would be interesting to study finite-size corrections for the classic de Gennes regime ($D \gg \ell_{\text{K}}^2/w_{\text{eff}}$) also. In this regime the universal scaling relation (3) does not hold. The observables are expected to scale differently for different ranges of L [16], and it remains to be determined how the finite-size effects depend on the parameters of the confined polymer system.

ACKNOWLEDGMENTS

Financial support from Vetenskapsrådet (grant number 2013-3992), from the Göran Gustafsson Foundation for Research in Natural Sciences and Medicine and the National Institutes of Health (R01-HG006851) is gratefully acknowledged. The computational work was carried out in part using computing resources at the University of Minnesota Supercomputing Institute.

[1] W. Reisner, J. N. Pedersen, and R. H. Austin, Rep. Prog. Phys. **75**, 106601 (2012).
[2] Q. He, H. Ranchon, P. Carrivain, Y. Viero, J. Lacroix, C. Blatché, E. Daran, J.-M. Victor, and A. Bancaud, Macromolecules **46**, 6195 (2013).
[3] D. R. Tree, Y. Wang, and K. D. Dorfman, Phys. Rev. Lett. **110**, 208103 (2013).
[4] Z. Benkova and P. Cifra, Biochem. Soc. Trans. **41**, 625 (2013).
[5] J. Z. Y. Chen, Macromolecules **46**, 9837 (2013).
[6] Y.-L. Chen, Biomicrofluidics **7**, 054119 (2013).
[7] L. Dai and P. S. Doyle, Macromolecules **46**, 6336 (2013).
[8] L. Dai, J. van der Maarel, and P. S. Doyle, Macromolecules **47**, 2445 (2014).
[9] D. Gupta, J. Sheats, A. Muralidhar, J. J. Miller, D. E. Huang, S. Mahshid, K. D. Dorfman, and W. Reisner, J. Chem. Phys. **140**, 214901 (2014).
[10] A. Muralidhar, D. R. Tree, Y. Wang, and K. D. Dorf-

man, J. Chem. Phys. **140**, 084905 (2014).
[11] E. Werner and B. Mehlig, Phys. Rev. E **90**, 062602 (2014).
[12] Y.-L. Chen, Y.-H. Lin, J.-F. Chang, and P.-K. Lin, Macromolecules **47**, 1199 (2014).
[13] C. Manneschi, P. Fanzio, T. Ala-Nissila, E. Angeli, L. Repetto, G. Firpo, and U. Valbusa, Biomicrofluidics **8**, 064121 (2014).
[14] D. Gupta, J. J. Miller, A. Muralidhar, S. Mahshid, W. Reisner, and K. D. Dorfman, ACS MacroLett. **4**, 759 (2015).
[15] B.-Y. Ha and Y. Jung, Soft Matter **11**, 2333 (2015).
[16] E. Werner and B. Mehlig, Phys. Rev. E **91**, 050601(R) (2015).
[17] Y. Wang, D. R. Tree, and K. D. Dorfman, Macromolecules **44**, 6594 (2011).
[18] P. Grassberger, Phys. Rev. E **56**, 3682 (1997).
[19] T. Prellberg and J. Krawczyk, Phys. Rev. Lett. **92**, 120602 (2004).
[20] V. Iarko, E. Werner, L. K. Nyberg, V. Müller, J. Fritzsche, T. Ambjörnsson, J. P. Beech, J. O. Tegenfeldt, K. Mehlig, F. Westerlund, and B. Mehlig, arXiv:1506.02241 (2015).
[21] A. V. Dobrynin, Macromolecules **39**, 9519 (2006).
[22] C.-C. Hsieh, A. Balducci, and P. S. Doyle, Nano Lett. **8**, 1683 (2008).
[23] D. Stigter, Biopolymers **16**, 1435 (1977).
[24] L. Nyberg, F. Persson, B. Åkerman, and F. Westerlund, Nucleic Acids Res. **41**, e184 (2013).
[25] B. Akerman and E. Tuite, Nucleic Acids Res. **24**, 1080 (1996).
[26] R. T. Kovacic, L. Comai, and A. J. Bendich, Nucleic Acids Res. **23**, 3999 (1995).
[27] T. Odijk, Phys. Rev. E **77**, 060901 (2008).
[28] R. van der Hofstad, F. den Hollander, and W. König, Probability Theory and Related Fields **125**, 483 (2003).
[29] P. C. Hiemenz and T. P. Lodge, *Polymer Chemistry* (CRC Press, Boca Raton, FL, 2007).
[30] A. Muralidhar and K. D. Dorfman, Macromolecules **48**, 2829 (2015).
[31] D. R. Tree, A. Muralidhar, P. S. Doyle, and K. D. Dorfman, Macromolecules **46**, 8369 (2013).
[32] L. Onsager, Ann. N. Y. Acad. Sci. **51**, 627 (1949).
[33] E. Werner, F. Persson, F. Westerlund, J. O. Tegenfeldt, and B. Mehlig, Phys. Rev. E **86**, 041802 (2012).
[34] A. Muralidhar, D. R. Tree, and K. D. Dorfman, Macromolecules **47**, 8446 (2014).